sustainability

MDPI

Article

Eco Rehabilitation at Real Scale of a Water Stream with Acid Mine Drainage Traits

Teresa Borralho [1,2,3,*], Renata A. Ferreira [1,2,4,*], Adelaide Almeida [1,2,3,5] and Anabela Durão [2,6,7]

1 Polytechnic Institute of Beja, Department of Technologies and Applied Sciences, Campus do IPBeja, Rua Pedro Soares, 7800-295 Beja, Portugal; maalmeida@ipbeja.pt
2 CREATE—Center for Sci-Tech Research in Earth System and Energy, Pole of Polytechnic Institute of Beja, 7800-295 Beja, Portugal; adurao@ipbeja.pt
3 FibEnTech-UBI—Fiber Materials and Environmental Technologies, Universidade da Beira Interior, 6201-001 Covilhã, Portugal
4 CERENA—Centre for Natural Resources and the Environment, Instituto Superior Técnico, University of Lisbon, 1049-001 Lisbon, Portugal
5 CENSE—Center for Environmental and Sustainability Research, NOVA School of Science and Technology, NOVA University Lisbon, Campus of Caparica, 2829-516 Caparica, Portugal
6 Polytechnic Institute of Beja, Department of Engineering, Campus do IPBeja, Rua Pedro Soares, 7800-295 Beja, Portugal
7 MARE—Marine and Environmental Sciences Centre, ARNET—Aquatic Research Network Associate Laboratory, NOVA School of Science and Technology, NOVA University Lisbon, 2829-516 Caparica, Portugal
* Correspondence: mtcarvalhos@ipbeja.pt (T.B.); renata.ferreira@ipbeja.pt (R.A.F.)

Abstract

The Água Forte (AF) stream located in the Southern Alentejo region (Portugal), is a tributary of the Roxo river. The AF stream has acid mining drainage (AMD) traits, which contributes to the degradation of the river's water quality and the adjacent soils. The use of ecological floating beds (EFBs) is an eco-rehabilitation strategy for polluted waters. This work aimed to evaluate the application of EFBs at real-scale as a water treatment system for the AF stream. Thus, three EFB, planted with *Vetiveria zizanioides* (3.3 $m^2 \cdot unit^{-1}$; density 40.5 $plants \cdot m^{-2}$), were placed on the stream. The water quality was monitored monthly, upstream (Inlet) and downstream (Outlet) of EFBs, from May 2020 to November 2021. With the use of the EFBs, the pH remained acidic, and the other main parameters showed average removal rates of around: 8% organic matter; 7% sulphates; 4% chlorides; 18% nitrogen, 30% copper, 29% zinc, 53% iron, and 10% manganese. Inlet and Outlet mass loads correlations showed high removal diversity. For the parameters under analysis, during the treatment period, the removal efficiency showed high variability due to the hydraulic conditions. The higher removal efficiencies were obtained for low-hydraulic retention times, except for heavy metals. Overall, EFBs showed some potential, but their efficiency was variable, highlighting the need for optimization under variable hydraulic conditions.

Keywords: nature-based solution; Água Forte stream; polluted river water real scale water treatment; ecological restoration; acid mining drainage

check for updates

Academic Editors: Meng Wang and Shanshan Li

Received: 16 September 2025
Revised: 2 November 2025
Accepted: 5 November 2025
Published: 11 November 2025

Citation: Borralho, T.; Ferreira, R.A.; Almeida, A.; Durão, A. Eco Rehabilitation at Real Scale of a Water Stream with Acid Mine Drainage Traits. *Sustainability* **2025**, *17*, 10064. https://doi.org/10.3390/su172210064

Copyright: © 2025 by the authors. Licensee MDPI, Basel, Switzerland. This article is an open access article distributed under the terms and conditions of the Creative Commons Attribution (CC BY) license (https://creativecommons.org/licenses/by/4.0/).

1. Introduction

The main problems found in surface water bodies are related to excess nutrients and metals. In fact, surface water courses in the "Baixo Alentejo" region (Portugal) are known to contain excess nutrients and/or metals due to farming practices, mining activities, and/or soil characteristics [1,2]. Additionally, the seasonal and annual variability of temperature and precipitation characteristic of the Mediterranean climate are exacerbated by climate

change. This leads to more flooding, more severe droughts, and greater toxicity of chemical contaminants in the environment due to the increase in their concentrations [3–5].

Mining is one of the human activities with the greatest impact on the environment. Its operations result in substantial changes to the surroundings, with direct and indirect consequences for various ecosystems. Water quality is impaired in several ways: by the mobilization and transport of sediment through runoff, by the atmospheric deposition of dust, and perhaps most critically, by acidification [6–8]. This acidification occurs mainly due to the leaching oxidative dissolution of exposed sulphide rocks, which release toxic substances (e.g., metals, sulphates). The change in water pH drastically affects aquatic communities [6–10].

The Água Forte (AF) stream, is located in the Southern Alentejo region (Portugal), with a length of around 11.7 km. It is a tributary of the Roxo river that crosses a large agricultural perimeter and receives runoff (Acid Mine Drainage, AMD) from the Aljustrel pyrite mine waters, located upstream. Consequently, the AF stream waters have a similar quality to an AMD with high concentrations of sulphates and chlorides, a low pH, and high concentrations of metals [11].

According to Nie et al. [12], water remediation from secondary tributaries should be prioritized because they significantly impact the subsequent receiving river watershed. In addition, improving water quality and reducing water stress is one of the measures mentioned by European Environment Agency [13] as necessary to increase the resilience of farms to extreme weather events. It is also crucial for protecting, restoring, and promoting the sustainable use of ecosystems and halting the loss of biodiversity [13]. Therefore, this type of solution appears to be a suitable option for improving the river's water quality, as is the case with the AF stream.

Several studies [14–19] report the use of Ecological Engineering-Based Processes (e.g., floating wetlands, artificial floating islands, hydroponic floating beds, ecological floating beds) for contaminant reduction, habitat conservation, water quality improvement, and green landscaping.

Ecological floating beds (EFBs) are nature-based solutions that use low-cost technology and offer easy maintenance [20]. They involve the deployment of artificial buoyant platforms designed to support the growth of emergent macrophytes. These structures are positioned directly on the water surface, allowing plant roots to remain fully or partially submerged, ensuring their unobstructed development and nutrient uptake [20]. Their pollutant removal is achieved through phytoremediation, which involves plant-mediated uptake of heavy metals, microbial degradation of organic contaminants, and nitrogen and phosphorus elimination via adsorption and sedimentation [21].

The EFBs have been extensively used in the treatment of eutrophic surface waters [20–22], wastewater [15,23,24], rainwater effluents [25,26], industrial effluents [26–29], and agricultural effluents [30,31]. It has been applied to the removal of heavy metals and radioactive compounds [15,26,32], as well as for the treatment of polluted rivers [33–35].

Macrophytes are crucial in this process due to their dense root systems, which contribute to promoting water circulation, establishing laminar flow between the surface and the bottom of the water column [34].

The choice of the macrophyte used in this work was based on previous pilot-scale studies, which tested two macrophytes (*Phragmites australis* and *Vetiveria zizanioides*). The *Vetiveria zizanioides* performed best in terms of purification capacity, mainly in removing heavy metals and sulphates [11]. It also showed great resistance when in contact with the water of the AF stream [11]. Although it is not native to Portugal, it is not considered an invasive species according to Portuguese Decree Law 92/2019 [36], and it is perennial.

Due to *Vetiveria zizanioides* characteristics, it is widely used in wastewater treatment [37]. Davamani et al. [38] achieved removal efficiencies of 81% for Chemical Oxygen Demand (COD), 66% for lead (Pb), and 64% for cadmium (Cd) in treated wastewater resulting from the treatment of industrial wastewater using this macrophyte in a hydroponic system. The use of *Vetiveria zizanioides* in mine rehabilitation by phytoremediation of mine runoff was reported by [39]. The plant shows potential for strategies that utilize root biomass as the primary absorption agent, proving effective in the translocation of Mn and copper (Cu) from the roots to the aerial parts [40].

The use of EFBs is a reliable technology for water purification [41,42], but questions remain about the requirements for real- and large-scale implementation. Previous studies have been conducted [20,22,43], but most have been carried out in confined environments (e.g., lakes, ponds, drainage sites). In relation to AMD treatment [8,44–46], reports artificial wetlands and EFBs with a programmed feeding system, regardless of flow type, with support matrices for plants or water [11,41,42,47,48]. The hydraulics and plant support of these types of systems differ from EFBs under analysis, which were performed with running-water flow. So, the present study evaluates the performance of EFBs at real-scale without controlled feeding and water with AMD traits.

With this exploratory work, the ability to use EFBs in river restoration was tested to improve the water quality with AMD traits at real-scale. For that, the pollution load at the AF stream was assessed from May 2020 to November 2021, considering: (1) the water physicochemical parameters, (2) the monthly monitoring of EFBs at upstream and downstream, and (3) the evaluation of the EFBs' performance.

2. Study Area Setting

2.1. Location of Água Forte (AF) Stream

The location of the AF stream is in southern Portugal, near the village of Aljustrel, and it is a tributary of the Roxo river (Figure 1). Both influence the water quality of the Roxo perimeter irrigation, and consequently, the Sado watershed. This stream is often temporary, so it exhibits high spatial variability during the wet (October–March) and dry (April–September) periods; consequently, the influent pollutants to the river are very closely related to the hydrological behaviour in the area [11].



Figure 1. Location of study area: (**a**) location of Aljustrel village; (**b**) general location of Água Forte (AF) stream; (**c**) detailed location of EFB https://earth.google.com/web, (accessed on 5 September 2025).

2.2. Meteorological Data

The climate in the study region is Mediterranean, characterized by warm and dry summers and wet winters [44]. Figure 2 presents meteorological data on precipitation (P) and maximum and minimum temperatures (Tmax and Tmin) during the study period at the Roxo meteorological station [49].

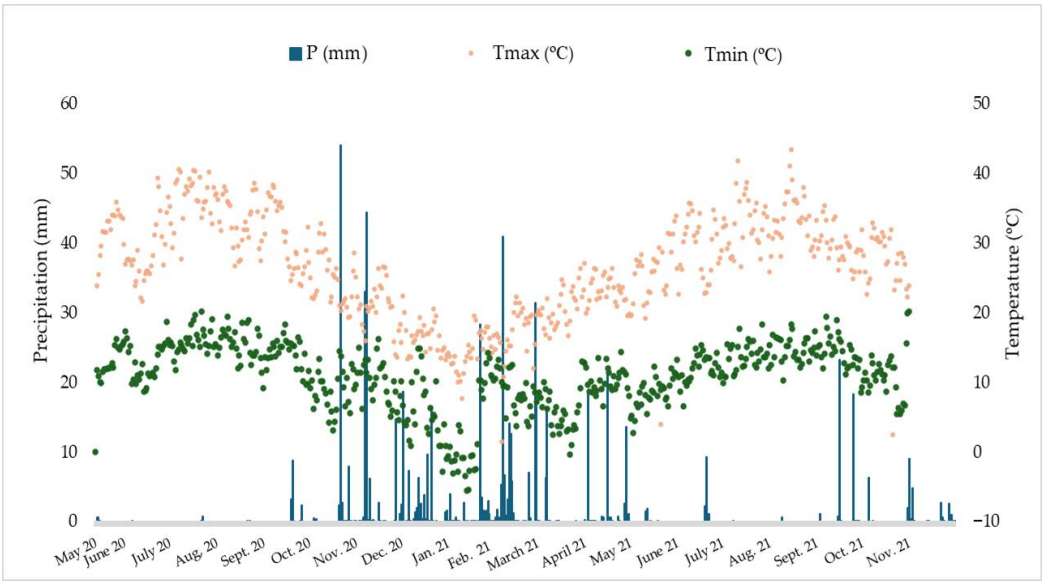

Figure 2. Daily precipitation and air temperatures (maximum and minimum), from May 2020 to November 2021.

As shown, precipitation was very low during spring (March–June) and was nonexistent during summer (June–August). The autumn and winter months were rainier, with periods of heavy rainfall occurring in November 2020 and February 2021. Temperatures followed the typical Mediterranean climate pattern, but Tmax and Tmin tended to be higher than historical records [50].

2.3. Physical and Chemical Characterization of Water Quality of AF Stream

The physical and chemical characterization of water quality in the AF stream are presented in Table 1. It shows, among others, acid pH, high electrical conductivity (EC), high organic matter (COD), low dissolved oxygen (DO) levels, high levels of metals, such as ferrous (Fe^{2+}), zinc (Zn^{2+}), copper (Cu^{2+}), and manganese (Mn^{2+}) ions, low concentrations of nitrogen (N) and phosphorus (P) nutrients, and high levels of chlorides (Cl^{-}) and sulphates (SO_4^{2-}), which are some of the stream features.

Table 1. Physical and chemical characterization of AF water stream (Mean ± SD, n = 6).

Parameter	Units	AF Water Quality [11]	Irrigation Water Quality [51]		Ecological State [52]
			RMV [1]	MAV [2]	
pH	Sorensen Scale	3.2 ± 0.1	6.5–8.4	4.5–9	6–9
T	°C	17 ± 2	-	-	-
Eh	mV	522 ± 19	-	-	-
EC	$\mu S \cdot cm^{-1}$ 20 °C	1813 ± 117	-	-	-
DO	$mg \cdot L^{-1}$	7 ± 1	-	-	≥5
COD	$mg \cdot L^{-1}$ O_2	30 ± 3	-	-	-
BOD_5	$mg \cdot L^{-1}$ O_2	4 ± 0	-	-	≤6

Table 1. *Cont.*

Parameter	Units	AF Water Quality [11]	Irrigation Water Quality [51]		Ecological State [52]
			RMV [1]	MAV [2]	
B^{3+}	$mg{\cdot}L^{-1}$	0.3 ± 0.1	0.3	3.7	-
PO_4^{3-}	$mg{\cdot}L^{-1}$	0.007 ± 0.001	-	-	-
TP	$mg{\cdot}L^{-1}$	0.009 ± 0.001	-	-	≤0.13
TN	$mg{\cdot}L^{-1}$	11± 2	-	-	-
NH_4^+	$mg{\cdot}L^{-1}$	9 ± 2	-	-	≤1
NH_3^-	$mg{\cdot}L^{-1}$	7 ± 1	50	-	≤25
SO_4^{2-}	$mg{\cdot}L^{-1}$	826 ± 321	575	-	-
Cl^-	$mg{\cdot}L^{-1}$	208 ± 21	70	-	-
F^-	$mg{\cdot}L^{-1}$	1.0 ± 0.0	1.0	15	-
TSS	$mg{\cdot}L^{-1}$	17 ± 1	60	-	-
TDS	$mg{\cdot}L^{-1}$	1238 ± 232	-	-	-
Zn^{2+}	$mg{\cdot}L^{-1}$	13 ± 2	2	10	-
Fe^{2+}	$mg{\cdot}L^{-1}$	8 ± 1	5	-	-
Cu^{2+}	$mg{\cdot}L^{-1}$	3 ± 1	0.20	5	-
Mn^{2+}	$mg{\cdot}L^{-1}$	7 ± 1	0.20	10	-

[1] RMV—Recommended Maximum Value. [2] MAV—Maximum Admissible Value.

The water quality assessment was carried out in accordance with Portuguese law, for irrigation purposes [51]. It revealed that the parameters pH, SO_4^{2-}, Cl^-, Cu^{2+}, Fe^{2+}, and Mn^{2+} exceed the Recommended Maximum Value (RMV), and the zinc value exceeds the Maximum Admissible Value (MAV). The pH and ammoniacal nitrogen (NH_4^+) parameters indicate a poor ecological state when evaluated in terms of physicochemical parameters [52].

3. Materials and Methods

3.1. EFBs Installation

The EFBs used consisted of a floating structure and a plant support system. This included a net layer of organic material (sisal) and a high-density polyethylene (HDPE) fluctuation support (Figure 3a,b). The macrophyte (*Vetiveria zizanioides*) was established with a density of 40.5 m^{-2} plants on three EFB units, each measuring 3.3 m^2 (3.3 m × 1.0 m). These were secured along the stream margins, Figure 3c, (GPS coordinates 37°56′39″ N 8°09′00″ W). The plants, which were about 20 cm long, were acclimated in water in the laboratory for about a month before planting.



Figure 3. EFBs structure and installation: (**a**) plant support; (**b**) floating structure; (**c**) field image [Authors' photos].

3.2. Experimental Procedure

Sampling Strategy

The monitoring was conducted between May 2020 and November 2021. However, in August 2020 and January 2021, sampling was not possible due to adverse meteorological conditions. The composite water samples were collected at two points: at upstream (Inlet) and downstream (Outlet) of the floating beds. The Inlet and Outlet collection sampling was conducted approximately 100 m before and after the EFBs installation, respectively. This was performed following Standard Methods of Analysis [53]. All sampling was made with an independent replicate.

The samples were transported to the laboratory in a cooler at 4 °C and immediately stored, following the requisites for water conservation for each parameter [53].

Water velocity was measured using a marker placed on the stream.

All physical parameters monitoring was performed, in situ. The parameters, pH, temperature (°C), electrical potential (Eh), electrical conductivity (EC), dissolved oxygen (DO), and total dissolved solids (TDS) were monitored twice a month using a multiparametric portable probe (HI9829, HANNA Instruments). The remaining (Fe^{2+}, Cu^{2+}, Mn^{2+}, Zn^{2+}, Cl^{-}, NH_4^{+}, COD, SO_4^{2-}, and total phosphorus (TP)) were monitored monthly in the laboratory and were determined according to Standard Methods for the Examination of Water and Wastewater [54].

3.3. Data Treatment

The flow rate was determined based on the surface area and water velocity of the channel stream.

The surface mass load (Inlet and Outlet) was calculated based on the concentrations of each parameter, flow rate, and total surface area of EFBs (Equation (1)) [55]:

$$\mathrm{Lo} = \frac{\mathrm{C} \times \mathrm{Q}}{\mathrm{A}} \quad (1)$$

where Lo—surface mass load ($kg \cdot m^{-2} \cdot d^{-1}$); C—concentration ($mg \cdot m^{-3}$); Q—flow rate ($m^3 \cdot d^{-1}$); and A—total surface area of EFBs (m^2).

The removal efficiency/parameter was calculated using the expression (Equation (2)) [55]:

$$\mathrm{R}(\%) = \frac{(\mathrm{In} - \mathrm{Out})}{\mathrm{In}} \times 100 \quad (2)$$

where R—Removal Efficiency; In—mass load at the Inlet sampling point; Out—mass load at the Outlet sampling point.

The hydraulic retention time (HRT) for total EFBs was calculated using (Equation (3)) [55]:

$$\mathrm{HRT} = \frac{\mathrm{A} \times \mathrm{h}}{\mathrm{Q}} \quad (3)$$

where Q—influent flow ($m^3 \cdot min^{-1}$); A—total beds surface area (m^2); h—water level (m).

The results for the monitored parameters were expressed as the mean of independent replicates. The correlations between the Inlet and Outlet data from different parameters were also assessed. All analyzed parameters were processed using Microsoft Excel statistical functions.

4. Results and Discussion

4.1. Hydraulic EFBs Characterization

Table 2 presents the hydraulic EFBs specifications of the installation during the treatment period. The variations in stream characteristics are demonstrated and may be related to rainfall and evapotranspiration, with a water level of 1.2 ± 0.3 m, a width of 8.9 ± 0.5 m, an average flow rate of 0.11 $m^3 \cdot s^{-1}$, ranging from 0.01 to 0.70 $m^3 \cdot s^{-1}$, and an HRT between 0.30 min and 19 min. The installation area of the EFBs was 10 m^2.

Table 2. Hydraulic EFBs characteristics installation.

Time (Months)	Water Level (m)	Width (m)	Flow Rate ($m^3 \cdot s^{-1}$)	HRT (min)
May 2020	1.0	9.0	0.07	2.6
June 2020	0.9	9.0	0.06	2.6
July 2020	1.0	8.9	0.05	3.7
August 2020	n.d.	n.d.	n.d.	n.d.
September 2020	1.4	9.0	0.03	2.2
October 2020	1.0	9.2	0.05	3.6
November 2020	1.0	9.3	0.09	1.8
December 2020	1.4	9.0	0.03	9.3
January 2021	n.d.	n.d.	n.d.	n.d.
February 2021	1.6	9.9	0.60	0.4
March 2021	2.1	9.2	0.20	1.8
April 2021	0.90	8.9	0.08	1.9
May 2021	1.2	8.9	0.01	19
June 2021	0.90	8.8	0.01	19
July 2021	1.0	8.9	0.01	19
August 2021	1.3	8.7	0.01	19
September 2021	1.1	9.0	0.05	3.7
October 2021	1.2	8.1	0.70	0.30
November 2021	1.1	7.4	0.04	4.5

n.d.—not determined.

4.2. Physical Parameters Monitoring

4.2.1. pH and Electrical Potential (Eh)

The temporal variation in pH and Eh from May 2020 to November 2021 is shown in Figure 4.

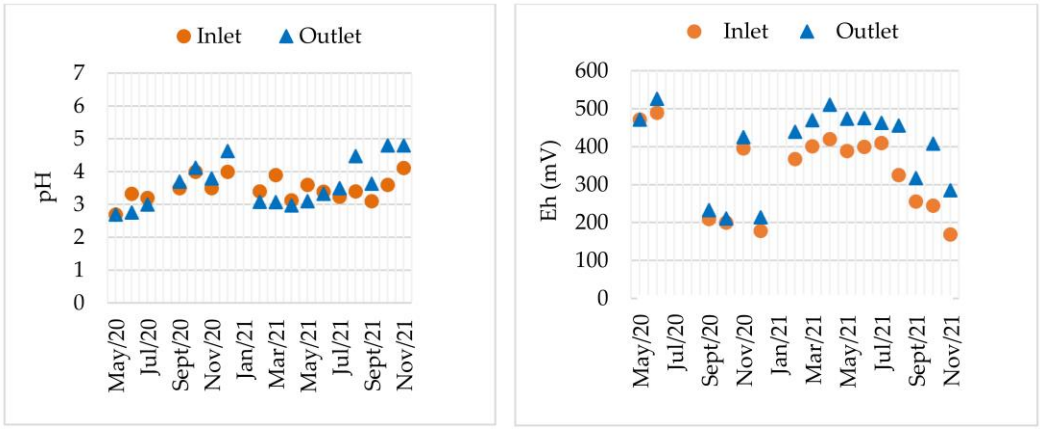

(**a**) (**b**)

Figure 4. Inlet and Outlet evolution: (**a**) pH; (**b**) electrical potential (Eh), from May 2020 to November 2021.

The Inlet pH values ranged mainly between 2.5 and 3.5, reflecting acidic conditions typical of AMD (Figure 4a). The Outlet consistently showed slightly higher values, ranging from 3.0 to 4.5, demonstrating the EFBs system's ability to increase the pH of the treated water. This behaviour has also been reported by [46]. In fact, the reduction in Fe-hydroxides or sulphate in the presence of bacteria sulphate reductor (SRB) is important in promoting pH increase [56]. A gradual upward trend over time was observed in both Inlet and Outlet measurements, suggesting the ecological maturation of the system.

Figure 4b revealed that Eh values ranged from ~170 mV to 530 mV. The Outlet values were generally higher than Inlet values, reflecting enhanced oxidizing conditions. Between May and November 2020, Eh declined significantly, suggesting more reducing conditions. From January to July 2021, values rose sharply, particularly at the Outlet, reaching nearly 500 mV (indicative of strongly oxidizing conditions). After July 2021, a progressive decline was observed, reaching 150 mV to 200 mV at the Inlet and 250 mV to 300 mV at the Outlet by November 2021. The Outlet consistently maintained higher Eh values, indicating that the EFB treatment enhanced oxygen availability and/or reduced organic matter [45]. However, the progressive decline in Eh after July 2021 suggests reduced treatment efficiency.

4.2.2. Electrical Conductivity (EC) and Total Dissolved Solids (TDS)

Figure 5 depicts the variation of EC (a) and TDS (b) during the treatment period. The elevated and relatively stable EC values at Inlet, ranging from 1300 $\mu S \cdot cm^{-1}$ to 2500 $\mu S \cdot cm^{-1}$, are high, but lower than those of a typical AMD [57], indicating a considerable concentration of dissolved ions. In this context, EC values are related to the presence of dissolved metals (e.g., Fe^{2+}, Cu^{2+}, Mn^{2+}, Zn^{2+}) and sulphates (SO_4^{2-}). The Outlet data revealed the same dynamic, and often with a positive treatment effect. Moreover, the results showed the existence of two trends in the behaviour of EC during the treatment: a consistent decline during May 2020 (2400 $\mu S \cdot cm^{-1}$) till December 2020 (1300 $\mu S \cdot cm^{-1}$), and after February 2021 (heavy precipitation), the values remained high until the end of treatment (2400 $\mu S \cdot cm^{-1}$ to 1765 $\mu S \cdot cm^{-1}$).

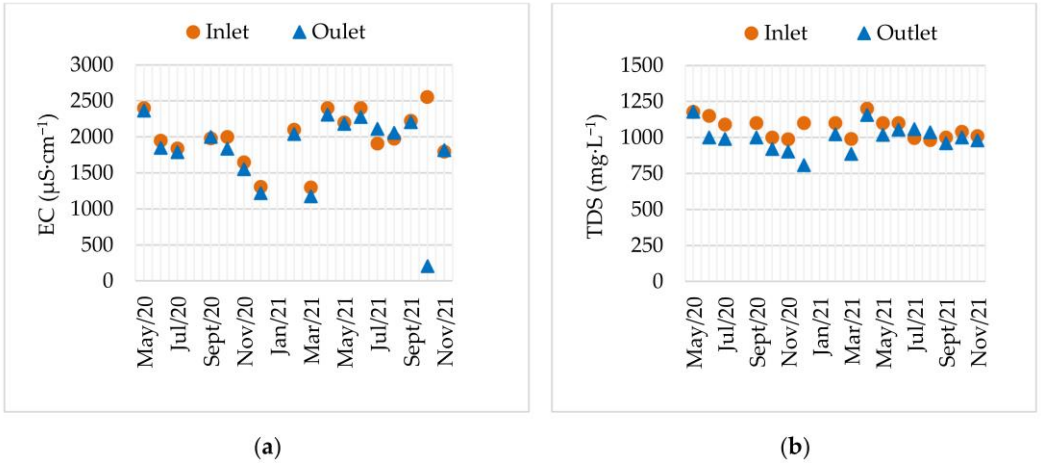

Figure 5. Inlet and Outlet evolution: (**a**) electrical conductivity (EC); (**b**) total dissolved solids (TDS), from May 2020 to November 2021.

The TDS represents the total amount of dissolved inorganic and organic solids in water and is related to the conductivity and salinity of the medium. Throughout the monitored period (May 2020 to November 2021), Inlet TDS values fluctuated between 980 $mg \cdot L^{-1}$ and 1200 $mg \cdot L^{-1}$, higher than the Outlet values, which oscillated between 950 $mg \cdot L^{-1}$ and 1050 $mg \cdot L^{-1}$. Although reductions in other environments (such as pilot-scale assays and constructed wetlands) are higher [58,59], they do not account for variability due to

treatment on a real-scale (i.e., seasonal, hydrological, etc.). Indeed, in those treatments, retention times are higher, and the support matrix can act as a filter.

4.2.3. Dissolved Oxygen (DO)

The DO is very important for water quality, due to its role in water bodies, reducing contamination mechanisms, and maintenance of aquatic life [14,60]. Therefore, regarding the evolution of this parameter in the AF stream (Figure 6), a low DO mass load was noticed at both monitoring points.

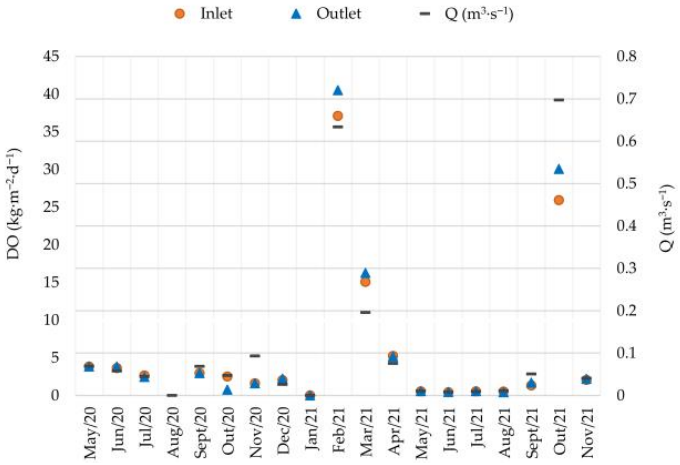

Figure 6. Evolution of the dissolved oxygen (DO) mass load at Inlet and Outlet sampling points from May 2020 to November 2021, and the respective flow rate (Q) measured on the AF stream.

Treatment with EFBs appears to have a modest effect on water oxygenation, although there was always a slight increase in its content at the Outlet of the treatment system. Two unexpected increases in oxygenation occurred when the streamflow rate reached maximum values due to stormy weather in February and October 2021, resulting in an Inlet load of 37 $kg \cdot m^{-2} \cdot d^{-1}$ and 26 $kg \cdot m^{-2} \cdot d^{-1}$ and an Outlet load of 41 $kg \cdot m^{-2} \cdot d^{-1}$ and 30 $kg \cdot m^{-2} \cdot d^{-1}$.

4.3. Chemical Parameters and Nutrients Monitoring

4.3.1. Chemical Oxygen Demand (COD)

To monitor the organic matter in the stream, which historically had high values, the COD parameter was used. As can be seen in Figure 7, during the treatment period, COD removal efficiencies were generally below 20%, except at low Inlet loads (<100 $kg \cdot m^{-2} \cdot d^{-1}$), where efficiencies reached ~40% to 50% (the highest efficiency obtained was 57%). For high Inlet loads (>200 $kg \cdot m^{-2} \cdot d^{-1}$), efficiency dropped markedly, suggesting system saturation or limited biodegradation capacity under high organic loads. These situations have occurred mainly during the months with the highest rainfall.

Moreover, a strong linear correlation (R^2 = 0.9986) was observed between the Inlet and Outlet COD loads. Overall, this analysis allowed us to infer that during the treatment period, the EFBs system was only able to remove, on average, 8% of organic matter from the AF stream. Results also showed that, on average, for each $kg \cdot m^{-2} \cdot d^{-1}$ of COD present upstream of the floating beds, 0.924 $kg \cdot m^{-2} \cdot d^{-1}$ were still present downstream.

The limited COD removal performance observed can be attributed to several factors intrinsic to AMD and EFBs, such as low pH and high dissolved metal concentrations, which create an environment hostile to heterotrophic microbial communities responsible for COD degradation [60]. The oxygen content and electrical potential present in the stream appear to be important factors in the process efficiency, as previously reported by [15].

The EFBs are more effective at enhancing oxygen transfer and promoting redox reactions for metal oxidation and precipitation [48] rather than degrading organic matter. Similar patterns have been reported in constructed wetlands and in EFBs treating wastewater with a low organic load but high metal content, where COD removal is secondary to metal removal [61].

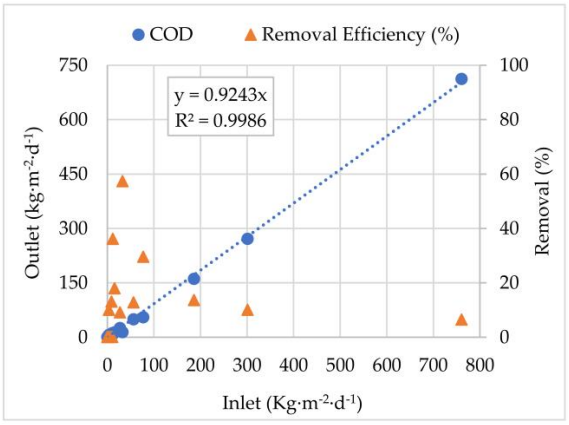

Figure 7. Inlet and Outlet mass load correlations and removal efficiencies for Chemical Oxygen Demand (COD) from May 2020 to November 2021.

4.3.2. Sulphates (SO_4^{2-}) and Chlorides (Cl^-)

The correlation between sulphates and chlorides loads and the removal efficiencies, at Inlet and Outlet, throughout the treatment, is presented in Figure 8.

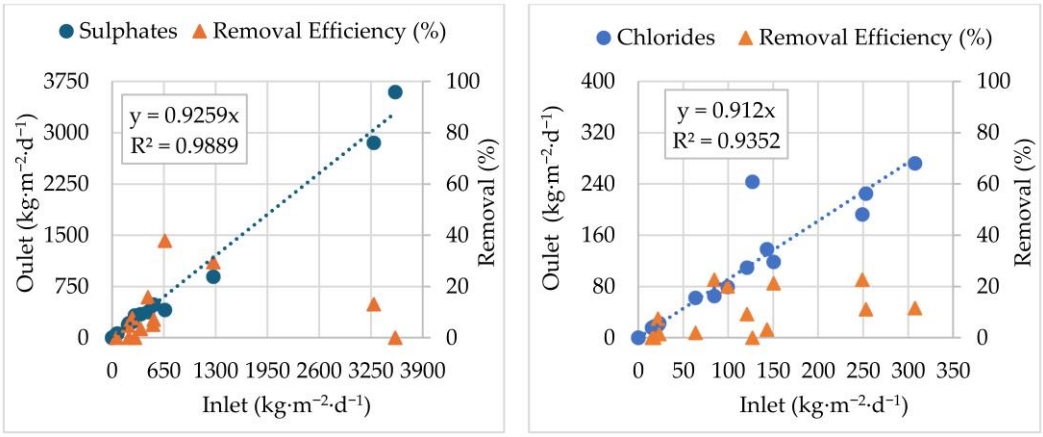

(**a**) (**b**)

Figure 8. Inlet and Outlet mass loads correlation and removal efficiencies: (**a**) sulphates (SO_4^{2+}); (**b**) chlorides (Cl^-), from May 2020 to November 2021.

A good linear correlation (R^2= 0.9889) between Inlet and Outlet sulphate loads was obtained (Figure 8a). Results also revealed that sulphate removal efficiency varied widely depending on the influent load: at low loads (<650 $kg \cdot m^{-2} \cdot d^{-1}$), removal efficiencies reached up to 40%; as the influent load increased above 2000 $kg \cdot m^{-2} \cdot d^{-1}$, removal efficiency declined, approaching zero at the highest tested values (~3500 $kg \cdot m^{-2} \cdot d^{-1}$). The EFBs operate predominantly under aerobic conditions, which restricts the activity of sulphate-reducing bacteria (SRB) [61], even though the removal efficiencies observed at low influent loads may be attributed to organic exudates from plant roots, which support limited SRB activity in localized anoxic niches within the biofilm [30].

Regarding chlorides (Figure 8b), the correlation between Inlet and Outlet indicates that Cl^- behaves predominantly as a conservative ion under the studied conditions, with

an average removal of only 4% from the AF stream during treatment. In fact, on average, for each kg·m^{-2}·d^{-1} of chlorides present upstream of the floating beds, 0.912 kg·m^{-2}·d^{-1} were still present downstream. Throughout the trial, the removal efficiency never exceeded 23%. The results indicate that the system has limited capacity for chloride removal. This was not a surprising result since Cl^- has high solubility, low reactivity, and a weak tendency to participate in precipitation or adsorption processes in natural treatment systems [48].

4.3.3. Ammoniacal Nitrogen (NH_4^+-N) and Total Phosphorus (TP)

Figure 9a depicts the correlation between mass load values of Inlet versus Outlet during the treatment period for NH_4^+-N and the corresponding removal efficiencies.

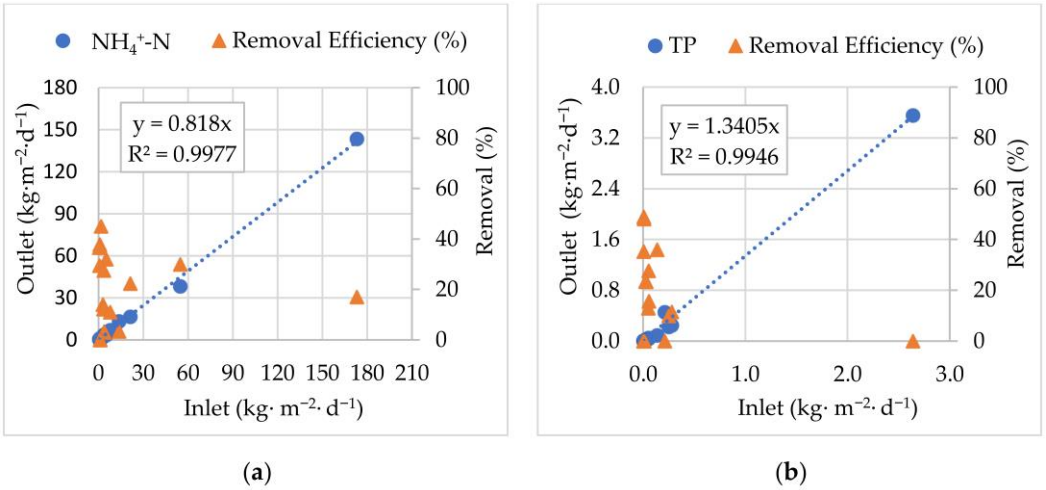

(**a**) (**b**)

Figure 9. Inlet and Outlet mass loads correlation and removal efficiencies: (**a**) ammoniacal nitrogen (NH_4^+-N); (**b**) total phosphorus (TP), from May 2020 to November 2021.

The good linear correlation (R^2 = 0.9977) observed, with the regression equation *y = 0.818x*, indicates that, on average, for each kg·m^{-2}·d^{-1}, of NH_4^+-N present upstream of the EFBs system, 0.818 kg·m^{-2}·d^{-1} was still present downstream, leading to 18% removal from the AF stream. During the treatment period, removal efficiencies exhibited variability across different Inlet loads. At lower values (<30 kg·m^{-2}·d^{-1}), removal efficiencies were generally high but scattered, reaching up to 50%. At higher loads (>100 kg·m^{-2}·d^{-1}) removal efficiencies stabilized at lower levels (~20%), suggesting a decline in treatment capacity under elevated loading conditions. The correlation between NH_4^+-N Inlet and Outlet mass loads underscores the performance of the system under varying nitrogen pressures. Although a consistent removal occurs, the system does not achieve complete elimination, which is in accordance with previous studies of nature-based nitrogen removal systems [57,58].

Regarding the TP results during treatment (Figure 9b), a good linear correlation (R^2 = 0.9946) between Inlet and Outlet loads was obtained. Results indicate that Outlet loads occasionally exceeded Inlet loads (y = 1.3405x). On average, for each kg·m^{-2}·d^{-1} of TP present upstream of the EFBs system, 1.3405 kg·m^{-2}·d^{-1} was present downstream. Phosphorus is a key nutrient influencing aquatic ecosystem health, and its excessive release contributes to eutrophication and water quality. Although AMD is generally characterized by low nutrient concentrations, phosphorus may still be present in mining influenced waters due to mineral weathering, runoff from surrounding soils, or anthropogenic inputs [62]. Phosphorus removal efficiencies were low. In some cases, due to low nutrient concentrations, phosphorus removal did not occur and even increased in some months. These results might be attributed to runoff and/or biomass decay [63–66]. To improve

removal efficiency, plants could be replaced, and/or an adsorption system, such as zeolites, could be incorporated into the EFBs [18].

In EFBs, the main mechanisms of phosphorus removal are physical, including complexation, sorption, filtration, precipitation, and fixation [30]. In acidic environments, its removal is complicated by competitive interactions with metals such as iron and aluminum, which can precipitate with phosphate under neutral-to-alkaline conditions but remain soluble under acidic pH [45]. Consequently, the AF stream water may have inhibited the removal of phosphorus.

4.4. Heavy Metals Monitoring

Heavy metals represent a significant concern regarding the characteristics of AMD effluents [5–7,9]. In fact, the AF stream, during the period of treatment, contained elevated concentrations of zinc (Zn^{2+}), (8 ± 6 mg·L^{-1}), copper (Cu^{2+}), (2 ± 1 mg·L^{-1}), iron (Fe^{2+}), (7 ± 5 mg·L^{-1}), and manganese (Mn^{2+}), (7 ± 2 mg·L^{-1}). Ecological floating beds typically remove these metals through different mechanisms, including phytoremediation, uptake and translocation by macrophytes, adsorption and immobilization on root surfaces, as well as microbial-mediated transformation and precipitation [28]. Figure 10 depicts the correlation between Inlet and Outlet mass load and removal efficiency, during the treatment period for (a) Zn^{2+}; (b) Cu^{2+}; (c) Fe^{2+}; (d) Mn^{2+}. The relation between the Inlet and Outlet of the different metal mass loads in the real-scale EFBs system provided insights into the metal removal dynamics at the AF stream.

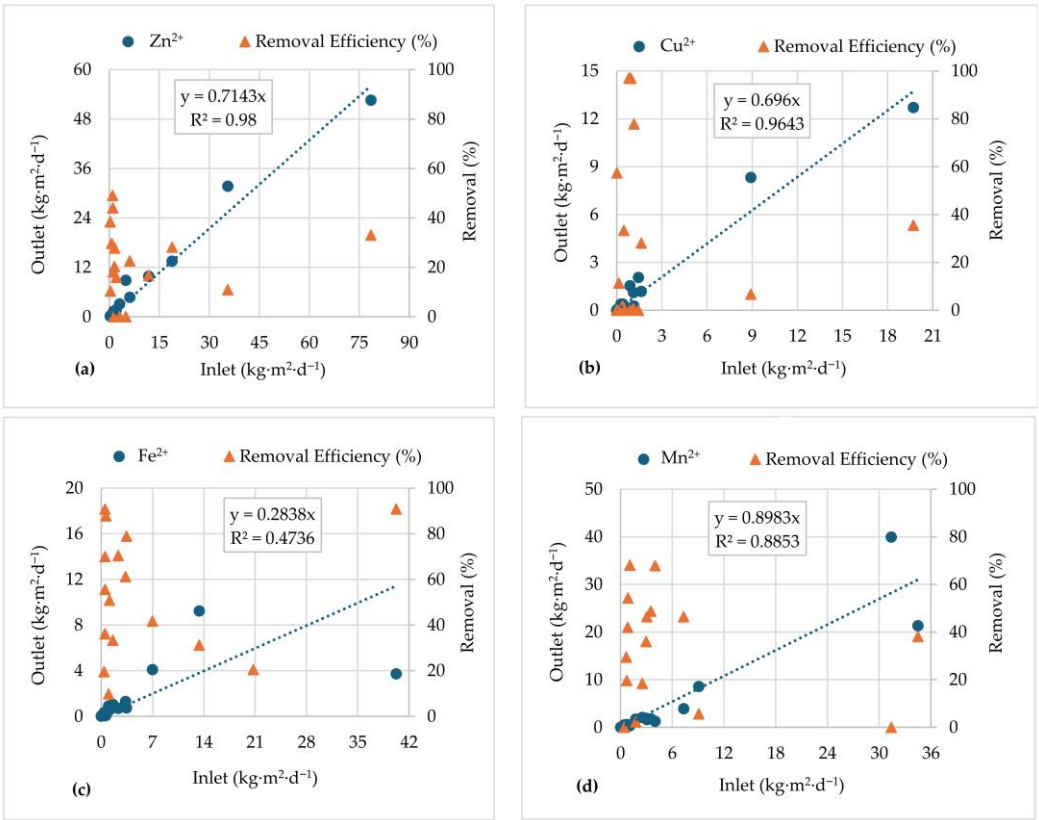

Figure 10. Inlet and Outlet mass loads correlation and removal efficiencies: (**a**) Zn^{2+}; (**b**) Cu^{2+}; (**c**) Fe^{2+}; (**d**) Mn^{2+}, from May 2020 to November 2021.

4.4.1. Zinc (Zn^{2+})

A good linear correlation ($R^2 = 0.98$) was obtained between Inlet and Outlet zinc loads (Figure 10a). During the treatment period, on average, for each kg·m^{-2}·d^{-1} of Zn^{2+} present upstream of the EFBs system, 0.714 kg·m^{-2}·d^{-1} was still present downstream, representing

an average of 29% removal from the AF stream. The removal efficiency obtained during the treatment reached higher values (up to 50%) mainly at lower influent loads, and some reduced efficiency was noticed at higher loads (between 10% and 20%).

When influent loads are low, removal pathways such as plant uptake, rhizofiltration, biofilm-mediated sorption, complexation, and precipitation are more active and effective, which accounts for the higher and more stable efficiency values observed [67]. On the other hand, when faced with high levels of loading, the ability of the EFBs to immobilize zinc might be surpassed due to the increase in flow and/or concentration levels. This could lead to a decrease in efficiency, even when there is significant removal, probably caused by the plant's uptake [27], mass transfer limitations [68], and hydraulic inefficiencies [69].

4.4.2. Copper (Cu^{2+})

The relation between Inlet and Outlet for Cu^{2+} mass loads in the real-scale EFBs system is shown in Figure 10b. The regression model (R^2 = 0.9643) indicates a positive correlation between Inlet and Outlet loads, suggesting that EFBs display predictable removal behaviour across a wide range of influent mass loads. The slope of 0.696 indicates that approximately 69.6% of this metal in the influent remained in the Outlet.

In the context of AMD, copper removal mechanisms are expected to involve multiple pathways: (i) biosorption to plant roots and associated biofilms, (ii) precipitation and co-precipitation with iron and manganese oxides under oxidizing conditions, and (iii) uptake and accumulation in macrophyte tissues [48,70].

The removal efficiency data show high variability, ranging from less than 20% to above 80%. Such fluctuations may reflect the temporal variations in hydraulic loading, retention time, plant growth dynamics, and seasonal changes in microbial activity within the rhizosphere. Previously, Sharma et al. [27] reported efficiencies between 20% and 50% for copper in industrial wastewater, while Bokhari et al. [70] achieved up to 70% removal using macrophyte species with high metal accumulation capacity. The mean Cu^{2+} removal efficiency observed in this study (~30%) is consistent with previous reports of metal attenuation in floating treatment wetlands.

4.4.3. Iron (Fe^{2+})

The performance of the EFBs in removing Fe^{2+} (Figure 10c) demonstrates a different trend compared to the other metals. The correlation analysis indicates that the relation between Inlet and Outlet iron loads is less predictable. The removal efficiencies reached high values, exceeding 85% both at lower and higher influent loads. The removal variability (from 10% to 91%) and the weak linear correlation (R^2 = 0.4736) suggest that the mechanisms of iron attenuation in EFBs are complex, despite the high efficiency percentages (on average, 53% of Fe^{2+} was removed during the treatment period).

Similar results have been reported [57,60,71], where Fe^{2+} removal is efficient but sensitive to variations in influent quality (pH, Eh, DO) and hydrological regime, requiring favourable conditions for oxidation, because an important removal mechanism of Fe^{2+} occurred by oxidation to Fe^{3+} and precipitation of the respective hydroxide. It has also been reported that the presence of neutrophilic iron-oxidizing bacteria, which live at the interface of aerobic and anaerobic zones, can contribute to iron oxidation in these passive systems [30,70].

4.4.4. Manganese (Mn^{2+})

The relation between Inlet and Outlet mass loads of Mn^{2+} during real-scale operation of EFBs treating AF stream water is presented in Figure 10d. From the correlation analysis, it was possible to determine that, during the observed EFBs operating window, on average,

only 10% of Mn^{2+} was removed. The obtained correlation coefficient (R^2 = 0.8853) suggests stable, load-driven behaviour. Results also showed that for each $kg \cdot m^{-2} \cdot d^{-1}$ of Mn^{2+} present upstream of the EFBs, 0.898 $kg \cdot m^{-2} \cdot d^{-1}$ was still present downstream. Moreover, the removal efficiency shows marked variability, from near-zero removal during high-load episodes to variable removal (from 30 to 68%) on lower loads. The low pH (Figure 4a) may be the main obstacle for the efficiency of the process, as stated by [29,60], which refers to the need for neutral–alkaline conditions for Mn^{2+} removal.

4.5. Hydraulic Retention Time (HRT) Treatment Influence

Since the EFBs treatment took place on a real-scale, weather conditions play a significant role in the hydraulic conditions of the stream, introducing variability in the pollutant loads, water chemistry, and water temperature. These fluctuations can often limit HRT, thereby affecting removal efficiencies. In fact, the relation between HRT and removal efficiencies provides empirical insights into how those can affect each other. This is crucial for evaluating the operational optimization of EFBs.

In Figure A1 (Appendix A), the influence of HRT on the removal efficiencies of (COD), (Cl^-), ($SO_4{}^{2+}$), ($NH_4{}^+$-N), (TP), and heavy metals (Cu^{2+}, Zn^{2+}, Fe^{2+}, and Mn^{2+}) is presented. The overall assessment of the results shows that for COD, $SO_4{}^{2+}$, and Cl^-, HRT > 5 min did not lead to appreciable removal efficiencies. However, removal efficiencies were also observed with HRT > 18 min for three of the studied metals: Zn^{2+}, Fe^{2+}, and Mn^{2+}.

To better understand the obtained data, a boxplot analysis was also done (Figure 11), dividing the HRT into three groups: Low (<2 min), Medium (2 ≤ min ≤ 6), and High (>6 min). Each boxplot shows the median, interquartile range, and individual data points (black dots).

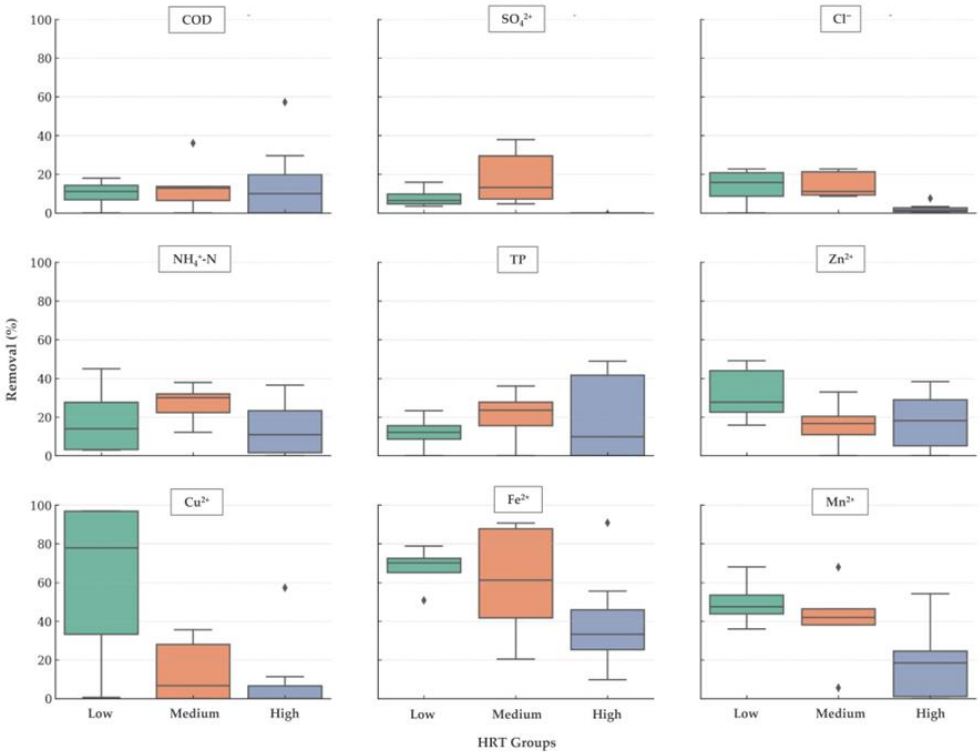

Figure 11. Removal efficiency by hydraulic retention time (HRT) group (Low: <2 min; Medium: 2 ≤ min ≤ 6; High: >6 min) for organic matter (COD), sulphates ($SO_4{}^{2+}$), chlorides (Cl^-), ammoniacal nitrogen ($NH_4{}^+$-N), total phosphorus (TP), and heavy metals (Cu^{2+}, Zn^{2+}, Fe^{2+}, and Mn^{2+}), from May 2020 to November 2021. The ♦ represents the analysis outliers.

Results show that the COD removal efficiency remains relatively stable across the different HRT groups, indicating limited sensitivity to retention time. For SO_4^{2-} and Cl^-, this analysis indicates an apparent decrease in removal efficiency for higher HRTs, suggesting ion release or reduced precipitation under longer residence times. In contrast, NH_4^+ and TP exhibit moderate variability, implying that HRT is not the primary controlling factor for nutrient removal. Moreover, the studied heavy metals exhibit diverse trends, with some decreasing at higher HRTs, possibly linked to redox changes and metal solubilization. High HRT also suggests stagnant water, i.e., very low flow rates.

Combined results (Figures 11 and A1) show that longer HRTs do not necessarily enhance overall EFBs treatment performance. Instead, there appears to be an optimal intermediate HRT at which organic matter degradation is balanced with limited metal release.

5. Conclusions

This manuscript reports the exploratory work carried out in situ at the AF stream, located in southern Portugal. This study presents a real-scale eco-rehabilitation intervention, offering practical insights into the effectiveness of this nature-based and sustainable strategy for mitigating heavy metal contamination in flowing water bodies.

For the parameters under analysis (COD, SO_4^{2+}, Cl^-, NH_4^+-N, TP, Cu^{2+}, Zn^{2+}, Fe^{2+}, and Mn^{2+}), the removal efficiency results showed high variability due to hydraulic conditions, which were exacerbated by the Mediterranean climate and climate change.

Higher removal efficiencies were observed at lower HRTs, except for TP, Zn^{2+}, Fe^{2+}, and Mn^{2+}. This behaviour is characteristic of dynamic systems, where it is not possible to control all the variables needed for the correct functioning of this type of treatment. In fact, this represents an additional difficulty in managing systems deployed at real-scale. The performance assessment of EFBs at real-scale, without controlled feeding and with water with AMD traits, contributes to the state of the art for nature-based solutions that protect, restore, and sustainably manage ecosystems. The EFBs solution showed some potential, but its efficiency was variable, highlighting the need for further work to clarify the mechanisms involved in the process.

Author Contributions: Conceptualization, T.B., A.A. and A.D.; methodology, T.B. and A.D.; formal analysis, T.B., R.A.F., A.A. and A.D.; writing, T.B., R.A.F. and A.D.; writing—review and editing, T.B., R.A.F. and A.D. All authors have read and agreed to the published version of the manuscript.

Funding: This research was funded by GreenEcoRoxo Operational Group (PDR2020-101-030894).

Institutional Review Board Statement: Not applicable.

Informed Consent Statement: Not applicable.

Data Availability Statement: The raw data supporting the conclusions of this article will be made available by the authors on request.

Acknowledgments: The authors would like to thank Fundação para a Ciência e Tecnologia (FCT, Portugal) through the strategic projects: CREATE (UIDB/06107/2023), FinEnTech.-UBI (UIDP/04292/2020), CERENA (UID/04028/2025), CENSE (Unit UID/04085), MARE (UIDP/04292/2020), and ARNET (LA/P/0069/2020). The authors would also like to thank all members of the GreenEcoRoxo Operational Group project.

Conflicts of Interest: The authors declare no conflicts of interest. The funders had no role in the design of the study; in the collection, analyses, or interpretation of data; in the writing of the manuscript; or in the decision to publish the results.

Appendix A

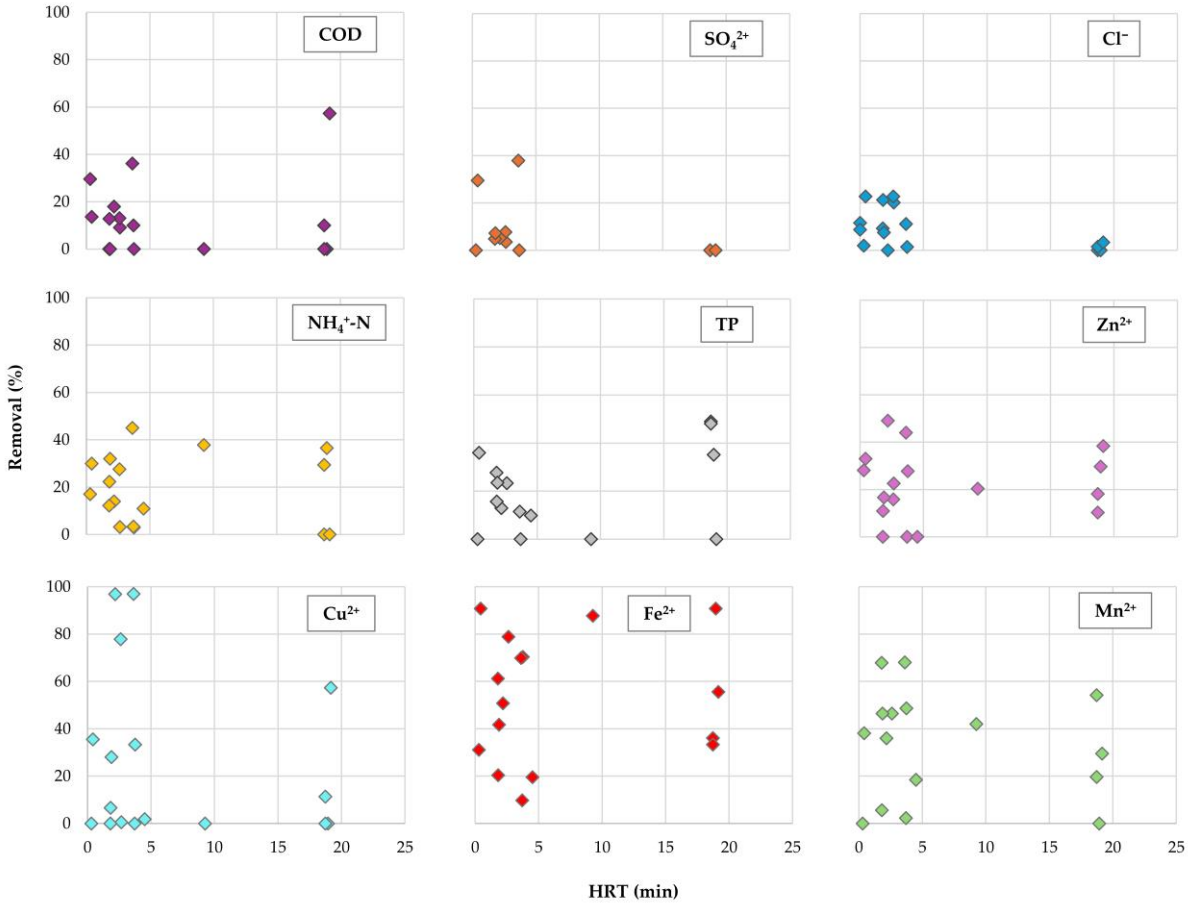

Figure A1. Hydraulic retention time (HRT) influence on the removal efficiency of organic matter (COD), sulphates (SO_4^{2+}), chlorides (Cl^-), ammoniacal nitrogen (NH_4^+-N), total phosphorus (TP), and heavy metals (Cu^{2+}, Zn^{2+}, Fe^{2+}, and Mn^{2+}), during the treatment period.

References

1. Borralho, T.; Durão, A. *Qualidade da Água da Albufeira do Roxo na Dinâmica dos Solos e Culturas Agrícolas (QARSC)*; Associação de Regantes do Roxo, Instituto Politécnico de Beja, Universidade de Évora: Aljustrel, Portugal, 2016; pp. 25–45.
2. Agência Portuguesa do Ambiente. Plano de Gestão da Região Hidrográfica do Sado e Mira (RH6) 2022–2027: Parte Sobre Qualidade da Água Superficial. *Lisboa: Agência Portuguesa do Ambiente.* 2022. Available online: https://tinyurl.com/apa-ambiente (accessed on 10 October 2025).
3. Lange, M.A. Climate Change in the Mediterranean: Environmental Impacts and Extreme Events. In *IEMed. Mediterranean Editions Yearbook 2020*; European Institute of the Mediterranean: Girona, Spain, 2020.
4. Tomaz, A.; Catarino, A.; Tomaz, P.; Fabião, M.; Palma, P. Patterns, Risks, and Forecasting of Irrigation Water Quality Under Drought Conditions in Mediterranean Regions. *Water* **2025**, *17*, 1783. [CrossRef]
5. Joseph, L.; Jun, B.M.; Joseph, R.V.F.; Park, C.M.; Yoon, Y. Removal of heavy metals from water sources in the developing world using low-cost materials: A review. *Chemosphere* **2019**, *229*, 142–159. [CrossRef] [PubMed]
6. Jiao, Y.; Zhang, C.; Su, P.; Tang, Y.; Huang, Z.; Ma, T. A review of acid mine drainage: Formation mechanism, treatment technology, typical engineering cases and resource utilization. *Process Saf. Environ. Prot.* **2023**, *170*, 1240–1260. [CrossRef]
7. Werner, T.T.; Bebbington, A.; Gregory, G. Assessing impacts of mining: Recent contributions from GIS and remote sensing. *Extr. Ind. Soc.* **2019**, *6*, 993–1012. [CrossRef]
8. Gupta, V.; Courtemanche, J.; Gunn, J.J.; Mykytczuk, N. Shallow floating treatment wetland capable of sulfate reduction in acid mine drainage impacted waters in a northern climate. *J. Environ. Manag.* **2020**, *263*, 110351. [CrossRef]
9. Grande, J.A.; Luís, A.T.; Santisteban, M.; Dávila, J.M.; Sarmiento, A.M.; Fortes, J.C.; Ferreira da Silva, E.; Córdoba, F. A common paragenesis and two A.M.D. pollution sources in the Iberian Pyrite Belt (SW Spain): Proposal of a natural attenuation model in the affected fluvial network. *J. Iber. Geol.* **2022**, *2*, 191–204. [CrossRef]

10. Oliveira, J. Fenómenos de Contaminação Metálica Associados à Evolução Supergénica de Paragéneses Sulfuretadas em Formações do Silúrico Caminha, N Portugal. Master's Thesis, Universidade do Minho, Caminha, Portugal, 2011. Available online: https://hdl.handle.net/1822/19721 (accessed on 10 July 2025).
11. Borralho, T.; Gago, D.; Almeida, A. Study on the Application of Floating Beds of Macrophites (*Vetiveria zizanioides* and Phragmites australis) in Pilot Scale for the Removal of Heavy Metals from AF Stream (Alentejo-Portugal). *J. Ecol. Eng.* **2020**, *21*, 153–163. [CrossRef]
12. Nie, Z.; Wu, X.; Huang, H.; Fang, X.M.; Xu, C.; Wu, J.Y.; Liang, X.Q.; Shi, J.Y. Tracking fluorescent dissolved organic matter in multistage rivers using EEM-PAAFAC analysis: Implications of the secondary tributary remediation for watershed management. *Environ. Sci. Pollut. Res.* **2016**, *23*, 8756–8769. [CrossRef]
13. European Environment Agency. *Nature-Based Solutions in Europe: Policy, Knowledge and Practice for Climate Change Adaptation and Disaster Risk Reduction*; Report No 01/2021; Publications Office of the European Union: Copenhagen, Denmark, 2021; ISBN 978-92-9480-362-7. [CrossRef]
14. Rome, M.; Happel, A.; Dahlenburg, C.; Nicodemus, P.; Schott, E.; Mueller, S.; Lovell, K.; Beighley, R.E. Application of floating wetlands for the improvement of degraded urban waters: Findings from three multi-year pilot-scale installations. *Sci. Total Environ.* **2023**, *877*, 162669. [CrossRef]
15. Arivukkarasu, D.; Sathyanathan, R. Floating wetland treatment an ecological approach for the treatment of water and wastewater—A review. *Mater. Today Proc.* **2023**, *77*, 176–181. [CrossRef]
16. Samal, K.; Kar, S.; Trivedi, S. Ecological floating bed (EFBS) for decontamination of polluted water bodies: Design, mechanism and performance. *J. Environ. Manag.* **2019**, *251*, 109550. [CrossRef]
17. Ge, P.; Chen, M.; Zhang, L.; Song, Y.; Mo, M.; Wang, L. Study on Water Ecological Restoration Technology of River. CCESEM IOP Conf. Series. *Earth Environ. Sci.* **2019**, *371*, 032025. [CrossRef]
18. Hossain, M.A.; Chowdhury, R. Remediation of Polluted River Water by Biological, Chemical, Ecological and Engineering Processes. *Sustainability* **2020**, *12*, 7017. [CrossRef]
19. Walker, C.; Tondera, K.; Lucke, T. Stormwater treatment evaluation of a constructed floating wetland after two years operation in an urban catchment. *Sustainability* **2017**, *9*, 1687. [CrossRef]
20. Lucke, T.; Walker, C.; Beecham, S. Experimental designs of field-based constructed floating wetland studies: A review. *Sci. Total Environ.* **2019**, *660*, 199–208. [CrossRef]
21. San Miguel, G.; Martín-Girela, I.; Ruiz, D.; Rocha, G.; Curt, M.D.; Aguado, P.L.; Fernández, J. Environmental and economic assessment of a floating constructed wetland to rehabilitate eutrophicated waterways. *Sci. Total Environ.* **2023**, *884*, 163817. [CrossRef]
22. Liang, Y.; Zhang, T.; Cui, W.; Kuang, Z.; Xu, D. Effects of Different Ecological Floating Bed Plant Assemblages on Water Purification and Phytoplankton Community Structure in Shallow Eutrophic Lakes: A Case Study in Lake Taihu. *Biology* **2025**, *14*, 807. [CrossRef]
23. Oktaviyani, D.; Pratiwi, N.T.M.; Krisanti, M.; Susanti, E. Floating treatment wetlands using *Vetiveria zizanioides* and *Heliconia psittacorum* in aquaculture wastewater treatment. IOP Conference Series. *Earth Environ. Sci.* **2023**, *1201*, 012074. [CrossRef]
24. Oliveira, G.A.; Colares, G.S.; Lutterbeck, C.A.; Dell'Osbel, N.; Machado, E.L.; Rodrigues, L.R. Floating treatment wetlands in domestic wastewater treatment as a decentralized sanitation alternative. *Sci. Total Environ.* **2021**, *773*, 145609. [CrossRef]
25. Yadav, S.; Kumar, J.; Malyan, S.K.; Singh, R.; Singh, O.; Goyal, V.C.; Singh, J.; Negi, R. Evaluating Pilot-Scale Floating Wetland for Municipal Wastewater Treatment Using *Canna indica* and *Phragmites australis* as Plant Species. *Sustainability* **2023**, *15*, 13601. [CrossRef]
26. Schück, M.; Greger, M. Plant traits related to the heavy metal removal capacities of wetland plants. *Int. J. Phytoremediat.* **2020**, *22*, 427–435. [CrossRef]
27. Sharma, R.; Vymazal, J.; Malaviya, P. Application of floating treatment wetlands for stormwater runoff: A critical review of the recent developments with emphasis on heavy metals and nutrient removal. *Sci. Total Environ.* **2021**, *777*, 146044. [CrossRef]
28. Dorafshan, M.M.; Abedi-Koupai, J.; Eslamian, S.; Amiri, M.J. Vetiver Grass (*Chrysopogon zizanoides* L.): A hyper-accumulator crop for bioremediation of unconventional water. *Sustainability* **2023**, *15*, 3529. [CrossRef]
29. Thakur, L.S.; Parmar, H.; Varma, A.K.; Chaurasia, A.K.; Mondal, P. Removal of Manganesee from synthetic wastewater by *Vetiveria zizanioides*. *Mater. Today Proc.* **2023**, *72 Pt 5*, 2687–2690. [CrossRef]
30. Mao, J.; Hu, G.; Deng, W.; Zhao, W.; Li, J. Industrial wastewater treatment using floating wetlands: A review. *Environ. Sci. Pollut. Res.* **2024**, *31*, 5043–5070. [CrossRef]
31. Hassan, E.A.; Tony, M.A.; Nabwey, H.A.; Awad, M.M. Ecologically engineered systems for treating agriculture runoff by integrating wastes into constructed wetlands. *Processes* **2023**, *11*, 396. [CrossRef]
32. Aryal, M. Phytoremediation strategies for mitigating environmental toxicants. *Heliyon* **2024**, *10*, 38683. [CrossRef]

33. Mohamed, A.R.N.E.; Kasem, A.M.M.A.; Ghanem, A.E.M.F.M.; Badry, M.O. Green solutions for heavy metal pollution in the aquatic environment of the Nile Islands: Cues from some submerged and emergent macrophytes. *Water Air Soil Pollut.* **2025**, *236*, 410. [CrossRef]
34. Bista, S.; Karki, B.K.; Maharjan, R. A Review Paper on Floating Treatment Wetlands: Working Principles and Applications for River Water Remediation. *J. Advanced College Eng. Manag.* **2025**, *10*, 13–30. [CrossRef]
35. Sun, S.; Zhang, M.; Gu, X.; He, S.; Tang, L. Microbial response mechanism of plants and zero valent iron in ecological floating bed: Synchronous nitrogen, phosphorus removal and greenhouse gas emission reduction. *J. Environ. Manag.* **2022**, *324*, 116326. [CrossRef]
36. *Portuguese Law-Decreto-Lei 92/2019, 1 Julho 2019, Assembleia da República. Diário da República, 1.ª Série—N.º 130*; INCM: Lisboa, Portugal, 2019; pp. 5688–5724. Available online: https://tinyurl.com/Decree-Law-1 (accessed on 10 July 2025).
37. Ramos-Arcos, S.A.; González-Mondragón, E.G.; López-Hernández, E.S.; Rodríguez-Luna, A.R.; Morales-Bautista, C.M.; Lagunas-Rivera, S.; López-Martínez, S. Phytoremediation Potential of *Chrysopogon zizanioides* for Toxic Elements in Contaminated Matrices. In *Biodegradation Technology of Organic and Inorganic Pollutants*; Mendes, K.F., Sousa, N., Mielke, K.C., Eds.; IntechOpen: London, UK, 2022. [CrossRef]
38. Davamani, V.; Parameshwari, C.I.; Arulmani, C.; John, J.E.J.; Poornima, R. Hydroponic phytoremediation of paperboard mill wastewater by using vetiver (*Chrysopogon zizanioides*). *J. Environ. Chem. Eng.* **2021**, *9*, 105528. [CrossRef]
39. Anning, A.K.; Akoto, R. Assisted phytoremediation of heavy metal contaminated soil from a mined site with Typha latifolia and *Chrysopogon zizanioides*. *Ecotoxicol. Environ. Saf.* **2018**, *148*, 97–104. [CrossRef] [PubMed]
40. Gautam, M.; Agrawal, M. Phytoremediation of metals using vetiver (*Chrysopogon zizanioides* (L.) Roberty) grown under different levels of red mud in sludge amended soil. *J. Geochem. Explor.* **2017**, *182*, 218–227. [CrossRef]
41. Suelee, A.L.; Hasan, S.N.M.S.; Kusin, F.M.; Yusuff, F.M.; Ibrahim, Z.Z. Phytoremediation Potential of Vetiver Grass (*Vetiveria zizanioides*) for Treatment of Metal-Contaminated. *Water Air Soil Pollut.* **2017**, *228*, 158. [CrossRef]
42. Kusin, F.M.; Has, S.N.M.S.; Nordin, N.A.; Mohamat-usuff, F.; Ibraim, Z.Z. Floating vetiver island (FVI) and implications for treatment system design of polluted running water. *Appl. Ecol. Environ. Res.* **2019**, *17*, 497–510. [CrossRef]
43. Pavlineri, N.; Skoulikidis, N.T.; Tsihrintzis, V.A. Constructed floating wetlands: A review of research, design, operation and management aspects, and data meta-analysis. *Chem. Eng. J.* **2017**, *308*, 1120–1132. [CrossRef]
44. Alvarenga, P.; Guerreiro, N.; Simões, I.; Imaginário, M.J.; Palma, P. Assessment of the Environmental Impact of Acid Mine Drainage on Surface Water, Stream Sediments, and Macrophytes Using a Battery of Chemical and Ecotoxicological Indicators. *Water* **2021**, *13*, 1436. [CrossRef]
45. Chen, J.; Li, X.; Jia, W.; Shen, S.; Deng, S.; Ji, B.; Chang, J. Promotion of bioremediation performance in constructed wetland microcosms for acid mine drainage treatment by using organic substrates and supplementing domestic wastewater and plant litter broth. *J. Hazard. Mater.* **2021**, *404*, 124125. [CrossRef]
46. Kiiskila, J.D.; Sarkar, D.; Panja, S.; Sahi, S.V.; Datta, R. Remediation of acid mine drainage-impacted water by vetiver grass (*Chrysopogon zizanioides*): A multiscale long-term study. *Ecol Eng.* **2019**, *129*, 97–108. [CrossRef]
47. Palihakkara, C.R.; Dassanayake, S.; Chulantha Jayawardena, C.; Senanayake, I.P. Floating Wetland Treatment of Acid Mine Drainage using *Eichhornia crassipes* (Water Hyacinth). *J. Health Pollut.* **2018**, *8*, 14–19. [CrossRef]
48. Marwa, A. Evaluation of wetland plants treatment potentials for acid mine drainage in Tanzania. *Nigerian J. Technol.* **2024**, *43*, 381–390. [CrossRef]
49. COTR SAGRA. Sistema Agrometeorológico Para a Gestão da Rega No Alentejo (Agrometeorological System for Irrigation Management in Alentejo). Available online: http://www.cotr.pt/servicos/sagranet.php (accessed on 1 August 2025).
50. IPMA. Drought Monitoring. Available online: https://www.ipma.pt/pt/oclima/observatorio.secas/ (accessed on 30 August 2025).
51. *Portuguese Law-Decreto-Lei 236/98, 1 Agosto 1998. Diário da República n º 176/98–I Série A*; Ministério do Ambiente: Lisboa, Portugal, 1998; pp. 3677–3722. Available online: https://tinyurl.com/Decree-Law-2 (accessed on 10 July 2025).
52. Critérios para a Classificação do Estado das Massas de Água Superficiais. Available online: https://tinyurl.com/58hmvkmc (accessed on 21 July 2025).
53. APHA. *Standard Methods for Examination of Water and Wastewater*, 22nd ed.; American Public Health Association: Washington, DC, USA, 2012.
54. APHA. *Standard Methods for Examination of Water and Wastewater*, 23rd ed.; American Public Health Association: Washington, DC, USA, 2017.
55. Kadlec, R.H.; Wallace, S. *Treatment Wetlands*, 2nd ed.; CRC Press, Taylor & Francis Group: Boca Raton, NY, USA, 2008; pp. 21–25.
56. Nagoum, I.; Edahbi, M.; Meliá, J.A.H.K.; Rodriguez, M.; Durães, N.; Pascual, B.A.; Salmoun, F. Passive Treatment of Acid Mine Drainage Effluents Using Constructed Wetlands: Case of an Abandoned Iron Mine, Morocco. *Water* **2025**, *17*, 687. [CrossRef]

57. Wang, X.; Wu, Y.; Chen, N.; Piao, H.; Sun, D.; Ratnaweera, H.; Maletskyi, Z.; Bi, X. Characterization of Oxidation-Reduction Potential Variations in Biological Wastewater Treatment Processes: A Study from Mechanism to Application. *Processes* **2022**, *10*, 2607. [CrossRef]
58. Gabr, M.E.; Salem, M.; Mahanna, H.; Mossad, M. Floating Wetlands for Sustainable Drainage Wastewater Treatment. *Sustainability* **2022**, *14*, 6101. [CrossRef]
59. Ali, M.; Aslam, A.; Qadeer, A.; Javied, S.; Nisar, N.; Hassan, N.; Hussain, A.; Ali, B.; Iqbal, R.; Chaudhary, T.; et al. Domestic wastewater treatment by *Pistia stratiotes* in constructed wetland. *Sci. Rep.* **2024**, *14*, 7553. [CrossRef]
60. Skousen, J.; Zipper, C.E.; Rose, A.; Ziemkiewicz, P.F.; Nairn, R.; McDonald, L.M.; Kleinman, R.L. Review of Passive Systems for Acid Mine Drainage Treatment. *Mine Water Environ.* **2017**, *36*, 133–153. [CrossRef]
61. Vymazal, J. Constructed wetlands for wastewater treatment: Five decades of experience. *Environ. Sci. Pollut. Res.* **2011**, *45*, 61–69. [CrossRef]
62. Nadagouda, A.N.; Varshney, G.; Varshney, V.; Charifa, A.; Hejase, C.A. Recent Advances in Technologies for Phosphate Removal and Recovery: A Review. *ACS Environ. Au* **2024**, *4*, 271–291. [CrossRef]
63. Kill, K.; Grinberga, L.; Koskiaho, J.; Mander, Ü.; Wahlroos, O.; Lauva, D.; Pärn, J.; Kasak, K. Phosphorus removal efficiency by in-stream constructed wetlands treating agricultural runoff: Influence of vegetation and design. *Ecol. Eng.* **2022**, *180*, 106664. [CrossRef]
64. Liu, W.; Yang, F.J.; Zhou, Y.L.; Li, Y.Y.; Liu, H.; Dan, A. Optimization and mechanism of phosphorus removal in plant-biofilm oxidation ditches: Plant uptake, iron plaque adsorption, and rhizosphere regulation. *Ecol. Eng.* **2023**, *196*, 106950. [CrossRef]
65. Shen, Y.T.; Hou, S.N.; Hu, S.L.; Miao, Y.Q.; Cui, H.; Zhu, H. Water purification capacity of ecological ditch: A systematic review and meta-analysis of influencing factors. *Ecol. Eng.* **2024**, *204*, 107280. [CrossRef]
66. Chu, X.; Zhao, F.; Liu, Y.; Xiao, J.; Ma, X.; Yan, Z. Phosphorus activation from phosphorus-saturated substrates by constructed wetlands plants: Performance and mechanism. *J. Water Process Eng.* **2025**, *71*, 107219. [CrossRef]
67. Boynukisa, E.; Schück, M.; Greger, M. Differences in metal accumulation from stormwater by three plant species growing in floating treatment wetlands in a cold climate. *Water Air Soil Pollut.* **2023**, *234*, 235. [CrossRef]
68. Barco, A.; Borin, M. Treatment performances of floating wetlands: A decade of studies in North Italy. *Ecol. Eng.* **2020**, *158*, 106016. [CrossRef]
69. Vo, T.K.Q.; Vo, T.D.H.; Ngatia, E.; Amulya, K.; Nguyen, N.K.Q.; Tran, P.Y.N.; Ninh, N.T.T.; Le, S.L.; Le, L.T.; Tran, C.S.; et al. Pilot and full-scale applications of floating treatment wetlands for treating diffuse pollution. *Sci. Total Environ.* **2023**, *899*, 165595. [CrossRef]
70. Bokhari, S.H.; Ahmad, I.; Ul-Hassan, M.M.; Mohammad, A. Phytoremediation potential of *Lemna minor* L. for heavy metals. *Int. J. Phytoremediat.* **2016**, *18*, 25–32. [CrossRef]
71. Okeleji, O.A.; Ioannidou, V.G. Seasonal Variation of Iron Removal in Coal Mine Water Discharge Lagoons and Constructed Wetlands. *Environ. Processes* **2025**, *12*, 29. [CrossRef]

Disclaimer/Publisher's Note: The statements, opinions and data contained in all publications are solely those of the individual author(s) and contributor(s) and not of MDPI and/or the editor(s). MDPI and/or the editor(s) disclaim responsibility for any injury to people or property resulting from any ideas, methods, instructions or products referred to in the content.